

A Review on BiOX (X = Cl, Br and I) Nano-/Microstructures for Their Photocatalytic Applications

Seema Garg^{1,*}, Mohit Yadav², Amrish Chandra³, and Klara Hernadi⁴

¹Amity Institute of Applied Sciences, Amity University, Noida 201313, UP, India

²Amity Institute of Nanotechnology, Amity University, Noida 201313, UP, India

³Amity Institute of Pharmacy, Amity University, Noida 201313, UP, India

⁴Department of Applied and Environmental Chemistry, University of Szeged, H-6720, Szeged, Rerrichtér 1, Hungary

In the recent past, bismuth oxyhalides (BiOX) have been widely used for the photocatalytic degradation of the organic pollutants and other environmental remediation because of their higher stability, economic viability, nontoxicity and effective charge separation. We begin with the review of the different approaches adopted so far for BiOX (X = Cl, Br, and I) synthesis and a study of their photocatalytic performances under UV and visible light towards the various organic as well as inorganic pollutants. Later on, a study on further enhancement of the efficiency of BiOX under UV and visible light irradiation using recent advancements would be presented. The new approaches involve controlled morphology by forming composite and hybrid materials with other semiconductors and also doping with other metals and nonmetals that would undoubtedly be beneficial in the interfacial charge transfer and efficient inhibition of the photo-generated species. Herein, we would also exploit the recent developments in the research strategies for enhancing photocatalytic activity of BiOX.

Keywords: Photocatalysts, Bismuth Oxyhalides, Visible Light, Heterostructures, Composites, Pollutants, Photodegradation, Photogenerated Species, Functionalization, Stability, Environmental Remediation.

CONTENTS

1. Introduction	280
2. Synthesis Methods and Photocatalytic Applications of BiOX	282
3. Heterogeneous Functionalization of BiOX with Other Semiconductors and Photocatalysts	285
4. Introduction of Defect and Solid Solutions	289
5. Summary and Outlook	290
Acknowledgment	291
References and Notes	291

1. INTRODUCTION

In the recent years, the rapid industrial development and population growth have led to increasing environmental pollution and serious energy shortages. With the growing chaos, the demand for environmental remediation, pollution control techniques and alternative energy supply have

attracted broad research interests. Even at low concentrations, some of the organic pollutants could be a severe threat to the environment and human health. Conventional wastewater techniques (precipitation, centrifugation, adsorption, filtration, etc.), remove the organic pollutants to some extent but can not completely eliminate these organic pollutants. Therefore, in order to overcome these limitations, an effective and green technique is required to degrade harmful pollutants into non-toxic substance without secondary pollution. With growing population, the reserves of fossil fuels are diminishing, and the energy supply is becoming a major issue for sustainable development. Hence the question arises, how the scientific means can be utilized to solve this issue. Now these days, the research interest is focused on using clean and renewable energy, such as ocean thermal energy, solar energy, tidal energy and wind energy. Semiconductor photocatalytic technology has emerged as a promising technique. It is also regarded as a green, efficient and effective solution

*Author to whom correspondence should be addressed.

for environmental remediation. Utilization of the solar energy by semiconductors for various applications such as photodegradation of toxic pollutants,^{1,2} water splitting,³⁻⁵ conversion of CO₂ into carbon sources⁶⁻⁸ is one of their key feature representing a promising solution for the environmental remediation.

Until now, TiO₂ has proven to be an excellent photocatalyst for the degradation of the organic pollutants. It has a wide band gap of 3.2 eV, and requires UV rays for the activation which accounts for less than 5% of the total solar energy; therefore, its photocatalytic

application gets limited under natural sunlight.⁹⁻¹⁴ Therefore to overcome these limitations and make optimum use of the solar light, visible light driven photocatalysts have been employed which are more effective and efficient in the presence of the sunlight. In this regard, various bismuth based semiconductors due to their low-toxicity and abundance on Earth have been reported such as BiOIO₃,¹⁵ Bi₄Ti₃O₁₂,^{16,17} Bi₂O₃,^{18,19} Bi₂WO₆,²⁰⁻²³ CaBi₂O₄,²⁴ BiVO₄,²⁵⁻²⁹ Bi₂O₂CO₃^{30,31} etc. These materials have shown promising photocatalytic activity for the photodegradation of the organic pollutants.



Seema Garg received her M.Sc. degree in Analytical Chemistry and Ph.D. in Chemistry from Agra University, Agra, UP, India. She had a long career of 18 years as a faculty and her research interests involve synthesizing nanoparticles using green methods for therapeutic applications, photocatalytic applications, solar cells and hydrogen generation etc. to provide efficient and affordable solution. She has to her credit 10 patents and a number of publications in journals of repute. She is on the reviewer and editorial board of many journals too. She is a Principal investigator in one of the Indo-Hungarian Project from Indian side, sanctioned in October 2016 which has been sponsored by DST, India—NRDIO, Hungary. She is supervising 3 students towards her doctoral degree and has supervised many post graduate students.



Mohit Yadav received his B.Sc. degree in Chemistry from Hansraj College, Delhi University in 2013 and M.Sc.–M.Tech. (Dual degree) in Nanotechnology from Amity Institute of Nanotechnology in 2016. Since December 2016, he joined Associate Professor Dr. Garg's group as a research fellow at Amity Institute of Applied Sciences. His current research concentrates on the synthesis of novel bismuth oxyhalides for environmental remediation.



Amrish Chandra started his professional career in 2002 after his post graduation from BIT, Mesra. He was fascinated by the applicability of non-invasive drug delivery technology and choose to work on Transdermal Drug Delivery System for his doctoral degree. He has to his credit 12 patents and has more than 50 national and international publications in recognized journals. His present research focus involves an integrative approach to harness the herbal diversity of the country, synthesize nanoparticles and develop effective formulations.



Klara Hernadi received her M.Sc. degree in chemistry from the University of Szeged in 1983, Ph.D./Candidate of Chemical Science from the Hungarian Sciences in 1993, and Doctor of Chemical Science in 2004 (HAS). She had short-term employments at Texas A&M University, at Facultés Universitaires Notre-Dame de la Paix (Namur Belgium) and at Ecole Polytechnique Federale de Lausanne (Switzerland). Currently she is the leader of Research group of Environmental Chemistry as a full professor at University of Szeged. Her current research interest covers various topics in the field of nanocrystalline materials (carbon nanotubes, hollow semiconductors, nanocomposites, etc.).

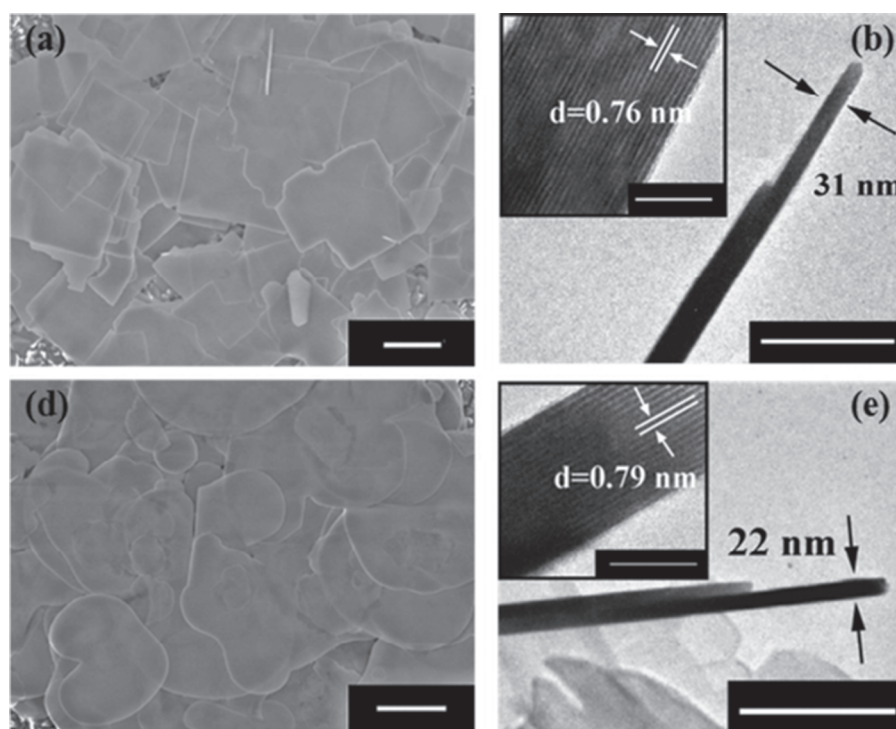


Figure 1. SEM images of (a) BiOBr-square, (d) BiOBr-circle (scale bar is 1 μm). Cross-sectional TEM images of (b) BiOBr-square, (e) BiOBr-circle (scale bar is 200 nm); insets are the HR-TEM images of the cross-sections, where both samples show layer structure along the c -axis (scale bar is 10 nm). Reprinted with permission from [111], H. Feng, et al., *ACS Appl. Mater. Interfaces* 50, 27592 (2015). © 2015, American Chemical Society.

One such category of bismuth related compounds is bismuth oxyhalides, BiOX (X = Cl, Br and I). They possess immense potential for their optical and electrical properties. Their composition comprises a layered structure containing $[\text{Bi}_2\text{O}_2]^{2+}$ slabs interleaved by double halogen atoms resulting in tetragonal matlockite geometry.^{32,33} This layered structure provides them enough space to polarize the orbitals and atoms resulting in induced dipoles that efficiently inhibit the separation of the electron-hole pair. In addition, these materials are negative {001} facet dominated which allows them to attain a high density of the terminated oxygen in the facets. They exhibit excellent photocatalytic applications towards NO oxidation, cationic organic dyes,^{34–38} in pigments,³⁹ pharmaceuticals,⁴⁰ catalysts,⁴¹ and gas sensors too⁴² etc. With the increasing size of the atom (Cl < Br < I), the band gaps of the BiOX compounds decrease in the same order, i.e., BiOCl ($\sim 3.1\text{--}3.5$ eV), BiOBr (~ 2.8 eV), and BiOI ($\sim 1.7\text{--}1.9$ eV) respectively. Hence, with decreasing bandgaps the photocatalyst requires less energy for the activation and allowing the maximum utilization of the visible light. At the same time, the question of fast recombination of the electron-hole pair comes into play; therefore, it has intrigued various researchers to synthesize BiOX nano-/microstructures to tune and enhance their photocatalytic performances.^{43–83} In congruence with the earlier reported reviews on BiOX,^{198–201} this review aims to study the recent developments in the synthesis and engineering of the BiOX compounds. Furthermore, the advancements

that were carried out in their structural composition and tuning with other materials in the form of composites and hybrid materials would be addressed.^{84–93}

2. SYNTHESIS METHODS AND PHOTOCATALYTIC APPLICATIONS OF BiOX

Different approaches have been adopted so far for the synthesis and enhancement of their photocatalytic activities. Among them, a wide range of the BiOX nano as well as microstructures such as 1D nanowires/rods,^{43–45} 2D nanosheets/plates,^{46–53} 3D hierarchical structures^{54–83} and thin films^{95–101} have been developed for the degradation of the organic pollutant. The 1D nanostructure with high aspect ratio and anisotropic layered structure efficiently inhibits the photogenerated electron-hole pair recombination and also can transform into 2D nanostructures. One such example of 1D nanostructure has been reported by Yuan et al.⁴⁴ where they synthesized BiOCl fibers via the solvothermal route. The as-prepared BiOCl fibers were able to achieve 75% mineralization of the methyl orange (MO) under UV radiations. Also, some other 1D materials involving PAN⁴³ and anodic aluminium oxide⁴⁵ have also been reported in the fabrication of the BiOCl nanofibres.

The 2D intrinsic lamellar structure of BiOX compounds with the resemblance to that of graphene allows the formation of the intra-electric field between $[\text{Bi}_2\text{O}_2]$ and halogen atoms that facilitates the transfer of the photogen-

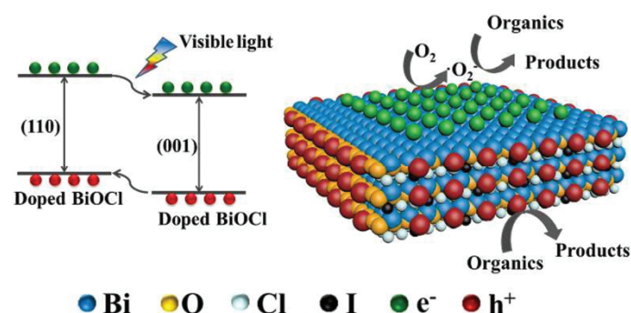


Figure 2. Schematic illustration of enhanced spatial carriers' separation. Reprinted with permission from [205], W. Liu, et al., *J. Mater. Chem. A* 5, 12542 (2017). © 2017, Royal Society of Chemistry.

erated electron-hole pair which results into efficient photocatalytic activity.^{94, 102–105} Some of the methods that are employed for the fabrication of 2D BiOX nanostructures include thermal annealing,⁵³ hydrothermal/solvothermal method,^{50–52} hydrolysis^{46–49} etc. Haifeng et al.¹¹¹ synthesized highly reactive {001} facets BiOBr nanosheets via the hydrothermal route as shown in Figures 1(a), (b), (d) and (e), respectively. From the Figures 1(a) and (d), two different morphologies of BiOBr nanosheets (i.e., square shaped and circle shaped) that were developed at different pH values can be seen. The thickness of the BiOBr nanosheets was revealed by TEM analysis as shown in Figures 1(d) and (e) and it was found to be 31 nm for square like and 22 nm for circle like. The BiOBr nanosheets were transformed from square-like to circle like nanosheets upon decrease in the pH values. The BiOBr circle-like

nanosheets exhibited excellent photocatalytic activity when compared to BiOBr square-like nanosheets and P25 toward the degradation of rhodamine B (RhB) under visible light irradiation. Ye et al.⁴⁶ synthesized BiOCl nanosheets by hydrolysis of a hierarchical flower like molecular precursor, i.e., $(\text{Bi}_n(\text{Tu})_x\text{Cl}_{3n})$, and high photocatalytic activity was observed which was about two times higher than P25 for the degradation of rhodamine B (RhB) under UV irradiation.

Transforming the 1D and 2D nanostructures into 3D nanostructures certainly has enhanced the device fabrication and tunable properties.^{106–110} The 3D engineering of the nanostructures has allowed more storage and conversion of the solar energy that provide the BiOX nanostructures much more efficient and enhanced utilization of the solar light, inhibition of the electron-hole pair and more reactive sites that facilitate their photocatalytic efficiency towards the organic pollutants. Among the various fabrication of BiOX nanostructures hydro/solvothermal and hierarchical techniques have proven to be more promising than other techniques.^{54–73} In a study by Tang et al.,⁶¹ 3D microspherical BiOBr structures were synthesized via ethylene assisted solvothermal route, the band gap of BiOBr was found to be 2.54 eV due to which it was able to perform much higher photocatalytic degradation of MO than BiOBr bulk plates under visible light irradiation. On the other hand, Zhang et al.,⁵⁴ used a

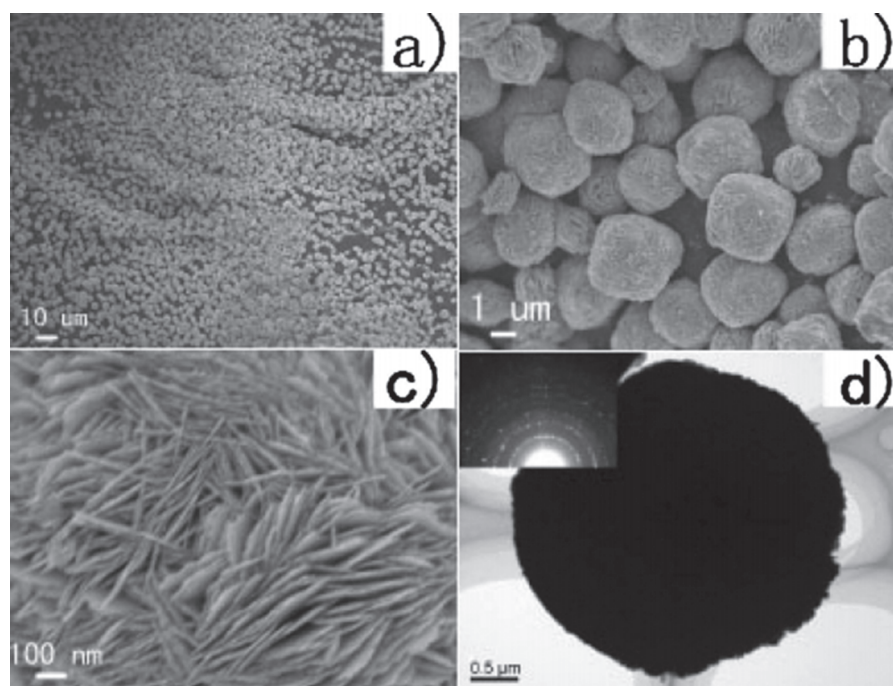


Figure 3. (a–c) SEM images of BiOBr 3D architectures at different magnifications, (d) TEM image of a single spherical architecture, and (inset) the SAED result of the product taken from the edge of the sphere. Reprinted with permission from [112], J. Zhang, et al., *ACS Chem. Mater.* 20, 2937 (2008). © 2008, American Chemical Society.

Table I. Different synthesis processes of bismuth oxyhalides and their photocatalytic performances towards the various pollutants.

Material	Synthesis method	Pollutant	% degradation of pollutant and time	Ref.
1D nanostructures				
BiOCl nanofibers	Electrospinning	RhB	~100% in 60 min.	[42]
BiOCl fibers	Solvothermal	MO	75% in 110 min.	[43]
BiOCl nanowire arrays	Sol-gel	RhB	~100% in 130 min.	[44]
2D nanostructures				
BiOCl plates	Hydrolysis	MO	~100% in 10 min.	[45]
BiOCl nanosheets	Hydrolysis	RhB	81.1% in 32 min.	[46]
BiOBr lamellar	Hydrolysis	RhB	~100% in 30 min.	[47]
BiOI, BiOBr, BiOCl nanosheets	Hydrolysis	Na-PCP (sodium pentachlorophenol)	95.9% in 60 min	[48]
BiOCl nanosheets	Hydrothermal	MO	99% in 45 min.	[50]
BiOCl nanoplates	Hydrothermal	RhB	~100% in 8 min.	[51]
BiOBr Lamellar	Hydrothermal	MO	96% in 120 min	[52]
BiOI nanosheets	Thermal annealing	RhB	~70% in 60 min.	[53]
3D nanostructures				
BiOI, BiOCl, BiOBr nanoplate microspheres	Solvothermal	MO	83% in 180 min.	[54]
BiOI, BiOCl, BiOBr hierarchical architectures	Solvothermal	MO	BiOI > BiOBr > BiOCl 100% in 60 min.	[55]
BiOCl porous nanospheres	Solvothermal	RhB	100% in 120 min.	[56]
BiOCl nanoflowers	Solvothermal	MO	100% in 10 min.	[57]
BiOCl hierarchical architectures	Solvothermal	RhB	100% in 60 min.	[58]
BiOCl self-assemblies	Hydrothermal	RhB	90.2% in 50 min.	[59]
BiOCl micro-flowers	Hydrothermal	RhB	99.3% in 15 min.	[60]
BiOBr nanoplate	Solvothermal	NO	30% in 10 min.	[62]
BiOBr microspheres	Solvothermal	Tertrabromo bisphenol A	100% in 15 min	[63]
BiOBr hollow microspheres	Solvothermal	RhB and chromium	100% in 15 min. and 90% in 20 min.	[64]
BiOBr microflowers	Solvothermal	MB	92.5% in 270 min.	[65]
BiOBr porous nanospheres	Solvothermal	RhB	100% in 105 min.	[66]
BiOBr microspheres	Microwave assisted solvothermal	Phenol	99% in 80 min.	[67]
BiOBr microspheres	Solvothermal	Micrococcus lylae	90% in 360 min.	[68]
BiOBr 3D microspheres	Solvothermal	Toluene	Conversion rate two-fold larger than P25	[69]
BiOBr microspheres	Solvothermal	RhB	95% in 40 min.	[70]
BiOBr mesoporous microspheres	Solvothermal	Bisphenol A	100% in 90 min.	[71]
BiOI hierarchical structure	Hydrothermal	MO	100% in 50 min.	[72]
BiOI hollow microspheres	Solvothermal	MO	92% in 180 min.	[73]
BiOI microflowers	Solvothermal	RhB	80% in 240 min.	[74]
BiOCl nanoflowers	Hydrolysis	RhB	100% in 50 min.	[75]
BiOCl sub-microcrystal	Hydrolysis	RhB	99.5% in 75 min.	[76]
BiOI microflowers	Direct precipitation	RhB	100% in 120 min.	[77]
BiOI microspheres	Direct precipitation	Tetracycline hydrochloride	94% in 120 min.	[78]
BiOCl hierarchical flowers	Sonochemical route	MO	90% in 60 min.	[79]
BiOBr fullerene like eggshells	Ultrasound reaction and heating synthesis	RhB	95% in 25 min.	[80]
BiOCl 3D desert roses	Refluxing method	RhB	100% in 20 min.	[81]
BiOI microspheres	Chemical bath	Phenol	97% in 240 min.	[82]
BiOCl 3D flowers	Solution oxidation process	RhB	100% in 80 min.	[83]
Thin films				
BiOCl nanosheets array	Solvothermal	MO	—	[95]
BiOCl thin film	Electrochemical route	MO	100% in 150 min.	[96]
BiOCl films	Hydrolysis	RhB	100% in 120 min.	[98]
BiOI thin films	Chemical vapor transport	RhB	90% in 120 min.	[99]

simpler solvothermal method involving ethylene glycol to synthesize BiOBr (~2.64 eV), BiOCl (~3.22 eV) and BiOI (~1.77 eV). The degradation of MO followed the order of BiOI > BiOBr > BiOCl respectively. Thin films

another important category of 2D nano/microstructures has attracted a lot of attention because of the easy handling, reclamation and separation.^{96–99} Mu and coworkers⁹⁵ fabricated a thin layer of vertical BiOCl nanosheet array

on a substrate of FTO (fluorine doped tin oxide) via the solvothermal route. It was observed that under UV irradiation, the BiOCl nanosheet showed much higher photocatalytic activity and durability as compared to P25 film towards the degradation of MO. In this context, Li et al.⁹⁷ in their study hydrolyzed the BiCl₃ in ethanol to fabricate BiOCl nanosheet on a stainless steel substrate, the BiOCl thin film showed significant superhydrophobicity and the water angle was able to reach upto 169 degrees.

Wenwen et al.²⁰² doped BiOCl nanosheets with different concentrations of iodine using hydrothermal method. The aim was to enhance the separation of photogenerated carriers by implementing doping strategy. BiOCl nanoplates were used as a model photocatalyst to investigate their effective carriers separation and photocatalytic activity. The enhanced spatial separation of photo-excited electrons and holes between (001) and (110) crystal facets of BiOCl nanoplates is achieved by doping. The enhanced photocatalytic efficiency was realized as shown in Figure 2.

Various attempts have been made to achieve the 3D hierarchical structures of BiOX as these structures are more intriguing because of their optimum use of the light in storing and exhibiting higher photocatalytic activity towards the pollutants. In this regard, Minqiang et al.,¹⁰⁹ in their work, synthesized BiOBr microspheres via solvothermal route assisted by polyethylene glycol 600 and 1-hexadecyl-3-methylimidazolium bromide as bromine source as well as the template. BiOBr microspheres showed much better photocatalytic activity than BiOBr nanoplates and P25 toward RhB under visible light. The following year, Chao et al.,¹¹⁰ in their study also synthesized 3D hierarchical BiOBr nanospheres by simple solvothermal route using ethylene glycol; pure crystalline tetragonal BiOBr microspheres were obtained which exhibited excellent photocatalytic activity under the visible light for the photodegradation of RhB with high stability. Jun et al.¹¹² demonstrated an ethylene glycol assisted solvothermal approach for the synthesis of 3D microspheres assembled by 2D nanosheets as shown in Figure 3. From the Figure 3(a), it can be seen that the as-prepared material comprises of a wealth of microspheres with varying diameters from 3 to 7 μm and good polydispersity of the spheres. Figures 3(b) and (c), indicated that the flower like microspheres consists of various nanosheets as petals. The nanosheets with 10 nm in size assembled together to form an open porous morphology. TEM analysis in Figure 3(d), also revealed the assembling of the nanosheets simultaneously and they continued to grow to form a 3D structure. Because of the novel 3D nano-/microstructure, BiOBr exhibited excellent photocatalytic activity towards the degradation of MO under visible light irradiation.

Apart from the ionic liquids,^{55, 56, 64, 66, 68, 73} various surfactants have also been utilized in the synthesis process of BiOX compounds such as CTAB (hexadecyltrimethylammonium bromide)^{62, 63, 65, 67, 69, 70} and PVP

(Polyvinylpyrrolidone)⁵⁹ etc. Among the various synthesis methods, the solvothermal route has been utilized mostly, in addition, some other processes have also been employed such as solution oxidation process,⁸³ hydrolysis,^{75, 76} refluxing method,⁸¹ sono-chemical route,^{79, 80} chemical bath⁸² and direct precipitation^{77, 78} etc. For example, Liquin et al.⁸² have reported the fabrication of MnO_x-BiOI heterogeneous photocatalyst to enhance the photocatalytic activity of BiOI and efficient charge separation. The photocatalytic performance of MnO_x-BiOI was compared to BiOI towards the photodegradation of RhB under visible irradiation, and it was found that the addition of MnO_x successfully enhanced the photocatalytic activity and also inhibited the recombination of the photogenerated electron-hole pair. Some of the recent developments on BiOX with their photocatalytic performances have been provided in the Table I given above.

3. HETEROGENEOUS FUNCTIONALIZATION OF BiOX WITH OTHER SEMICONDUCTORS AND PHOTOCATALYSTS

In order to further enhance the photocatalytic activity of BiOX compounds, various attempts have been made to hybridize BiOX by varying the composition and tuning the band gap in association with other materials including semiconductors,^{113–145} metals,^{146–153} sensitizers^{154–163} and organic materials²⁰² etc. The main concern associated with heterogeneous photocatalysis is the limitation to perform on a large scale practical applications. Association of an individual semiconductor with other semiconductor results into a much more fascinating heterostructure that is capable of inhibiting the recombination of electron-hole pair through effective interfacial charge transfer and also require less energy upon irradiation, these traits allows maximum utilization of the light ultimately resulting into higher photocatalytic performance towards the pollutants. BiOCl being a member of BiOX group has a large band gap, unlike BiOBr and BiOI, BiOCl is UV activated, hence under performs under visible light, in this context associating BiOCl with suitable band gap semiconductors results into a composite with narrow band gap which allows it to show maximum photocatalytic activity under visible light. Lee et al.¹⁴⁵ in 2011, by the process of chemical etching of Bi₂O₃ by HCl synthesized a heterojunction of BiOCl/Bi₂O₃, where Bi₂O₃ acted as a sensitizer under visible light and BiOCl as the main photocatalyst. The combination showed excellent photocatalytic activity towards 2-propanol and 1,4-terephthalic acid as compared to that of P25. Apart from these various other composites have been listed in the table given below which have turned out be an excellent heterogeneous photocatalyst under visible light. BiOX being a *p*-type semiconductor, allow the construction of *p-n* junction photocatalyst. In this regard, BiOI has gained a lot of popularity because of its low band gap

Table II. Some recent BiOX based hybrids and their enhanced photocatalytic applications.

Functionalized material	Synthesis method	Pollutant	% degradation of pollutant and time/enhanced efficiency	Ref.
Semiconductor composites				
BiOBr/ZnFe ₂ O ₄	Precipitation deposition	MO	100% in 40 min.	[113]
Bi ₄ Ti ₃ O ₁₂ /BiOI	Successive ionic layer adsorption reaction	RhB and phenol	Higher degradation as compared to Bi ₄ Ti ₃ O ₁₂	[114]
BiOI/Bi ₂ O ₃	Chemical etching	Phenol	3.9 times higher than Bi ₂ O ₃	[115]
BiOI/Bi ₂ O ₂ CO ₃	Co-precipitation method	RhB	8 times higher than BiOI	[116]
BiOI/(BiO) ₂ CO ₃	Chemical etching	MO	Enhanced MO degradation as compared to BiOI and (BiO) ₂ CO ₃	[117]
BiOI/ZnTiO ₃	Precipitation deposition	RhB	9.8 and 11.1 higher than BiOI and ZnTiO ₃	[118]
BiOI/ZnWO ₄	Chemical bath	MO	86% in 240 min.	[119]
BiOI/ZnO	Chemical bath	MO	Enhanced degradation than BiOI and ZnO	[120]
BiOI/TiO ₂	Impregnating hydroxylation	MO	3 times higher than BiOI	[121]
BiOI/TiO ₂	Soft-chemical method	MO	95% in 120 min	[122]
BiOBr/g-C ₃ N ₄	Solvothermal synthesis	RhB	87% in 30 min.	[123]
BiOBr/C ₃ N ₄	Deposition-precipitation	RhB	Higher degradation rate than BiOBr and C ₃ N ₄	[124]
BiOI/BiOBr	Deposition-precipitation	MO	Higher degradation than that of BiOI and BiOBr	[125]
BiOBr/bismuth oxyhydrate	Hydrothermal	RhB	10.7 times higher than that of P25	[126]
BiOBr/Bi ₂ WO ₆	Hydrothermal	RhB	100% in 40 min.	[127]
BiOBr/AgBr	Co-precipitation	RhB	100% in 30 min.	[128]
BiOI/AgI	Ion exchange	RhB	7.8 and 3 times higher than that of BiOI and AgI	[129]
BiOI/AgI	Ion exchange	2,4-DCP (2,4-dichlorophenol)	3 times higher than that of the same synthesized by chemical bath	[130]
BiOI/AgI	Chemical bath	Phenol	3 times higher than BiOI	[131]
BiOI/Bi ₂ S ₃	Ion exchange	MO	81.9% in 300 min.	[132]
BiOCl/Bi ₂ S ₃	Ion exchange	RhB	Higher than that of BiOCl, Bi ₂ S ₃ and P25	[133]
BiOCl/Bi ₂ S ₃	Ion exchange	2,4-DCP	13 times higher than that of N doped P25	[134]
BiOI/BiOCl	Solvothermal	Bisphenol A	4 times higher than BiOI	[135]
BiOCl/BiOI	Hydrothermal	MO and RhB	Higher degradation of MO and RhB than that of BiOI and BiOCl	[136]
BiOCl/BiOBr	Solvothermal	RhB	Higher degradation rate than BiOCl and BiOBr	[137]
BiOCl/ bismuth oxyhydrate	Hydrothermal	RhB	5 times higher than that of P25	[138]
BiOCl/BiNbO ₄ /TiO ₂	<i>In situ</i> precipitation	RhB	Higher degradation rate than BiNbO ₄ and BiOCl	[139]
WO ₃ /BiOCl/Bi ₂ O ₃	Chemical etching and incipient wetness	2-propanol	1.3 times more degradation rate than N-doped TiO ₂	[140]
BiOCl/NaBiO ₃	Chemical etching	RhB	Higher degradation rate than pure BiOCl and NaBiO ₃	[141]
Fe ₃ O ₄ /BiOCl	Phase-transfer	RhB	100% in 40 min.	[142]
WO ₃ /BiOCl	Impregnation	RhB	40 times higher degradation than P25	[143]
BiOCl/Bi ₂ O ₃	Chemical etching	2-propanol	5.7 times higher degradation rate than P25	[145]
Hybrid or co-catalysts				
BiOCl/graphene	Solvothermal	Methyl benzene	2 times higher degradation rate than BiOCl	[154]
BiOI/graphene	Hydrothermal	MO	6 times higher degradation rate than BiOI	[155]
BiOBr/graphene	Solvothermal (microwave assisted)	MO	~100% in 80 min.	[156]
BiOBr/graphene	Solvothermal	RhB	3 times higher degradation rate than BiOBr	[157]
BiOBr/graphene	Solvothermal	NO	2 times higher degradation rate than BiOBr	[158]
BiOI/MWCNT	Solvothermal	AOII (acid orange II)	~100% in 180 min	[159]
BiOI/[Bmim]I IL	Chemical bath	MO	Enhanced degradation rate than BiOI	[160]
MnO _x /BiOI	Photo-deposition	RhB	78.8% in 30 min.	[161]
BiOCl/phthalocyanine copper	Liquid coating	–	76 times higher photocurrent density than BiOCl under simulated light	[162]
BiOCl/Bi _n (Tu) _x Cl _{3n}	Hydrolysis	RhB	13 times higher degradation rate than BiOCl	[163]

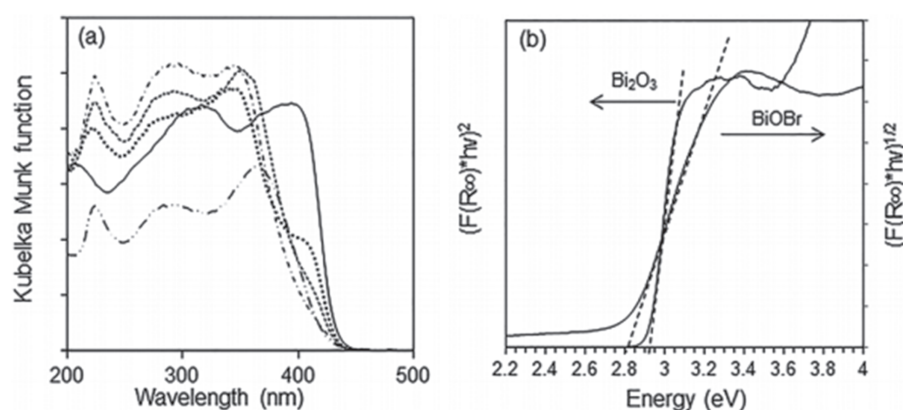


Figure 4. (a) Diffuse reflectance spectra of (—) Bi₂O₃, (---) BiOBr, BiOBr/Bi₂O₃ composites with (...) 12%, (-.-) 57% and (-.-) 85% BiOBr and (b) determination of absorption edge energies for Bi₂O₃ and BiOBr. Reprinted with permission from [206], A. Han, et al., *RSC Adv.* 7, 145 (2017). © 2017, Royal Society of Chemistry.

among the group. When associated with other *n*-type wide band gap semiconductors it acts as a visible light sensitizer resulting in high photocatalytic activity. Until now, a lot BiOI based *p-n* junction photocatalysts have been reported which are listed in the Table II given above. In 2012, Hefeng and coworkers¹²³ reported a novel BiOI/AgI composite that performed far superior photocatalytic activity towards MO and phenol as compared to that of pure BiOI and AgI under visible light irradiation. The band gap calculations revealed that both AgI and BiOI followed type II heterostructure with staggered band gap potentials. It was found that although the AgI/BiOI composite is quite stable but there were poor adhesion and dispersity between the AgI nanoparticles and BiOI nanoplates, therefore to overcome these limitations, an optimized approach was followed to synthesize 3D hierarchical AgI/BiOI hybrid system in which there was uniform dispersion of AgI nanoparticles on BiOI nanoplates. The AgI/BiOI hybrid shown excellent photocatalytic activity towards the degradation of 2,4-DCP as compared to AgI, BiOI and AgI/BiOI composite under visible light.

Aijuan et al.²⁰³ mitigated the high rate of electron-hole recombination by synthesizing BiOBr/Bi₂O₃ composite. Bi₂O₃, BiOBr and the composites all absorb in the

visible light region with the absorption edge between 380 and 470 nm (Fig. 4(a)). For Bi₂O₃, the best linear fit was obtained with $\eta = 1/2$, in agreement with a direct-allowed electron transition of the material, and the E_g was deduced to be 2.92 eV (Fig. 4(b)). Because the band gap transition in BiOBr is indirect, a linear fit was obtained with $\eta = 2$ and the E_g was calculated to be 2.82 eV. Despite the wider band gap in Bi₂O₃, its absorption in the visible light region of 400–500 nm is stronger than that of BiOBr due to the direct excitation of electrons. The absorption of BiOBr/Bi₂O₃ composites decreased with BiOBr content, and these materials have two band gaps between 2.82 and 2.92 eV. Hongwei et al.,¹⁶⁴ fabricated BiVO₄/BiOI core/shell heterostructure by facile *in situ* deposition route. The charge separation process in the *p-n* junction of BiVO₄/BiOI can be seen in Figure 5. Before contact, the Fermi level in *p*-type BiOI lies near to the valence band, while in *n*-type BiVO₄ it is closer to the conduction band. In addition, the nested band structure of both these photocatalysts inhibits the effective separation of photogenerated electron-hole pair. After contact, the BiOI nanosheets assemble BiVO₄ and forms a *p-n* heterojunction such that the Fermi level of BiVO₄ moves down while the Fermi level of BiOI moves up to set up an equilibrium state with

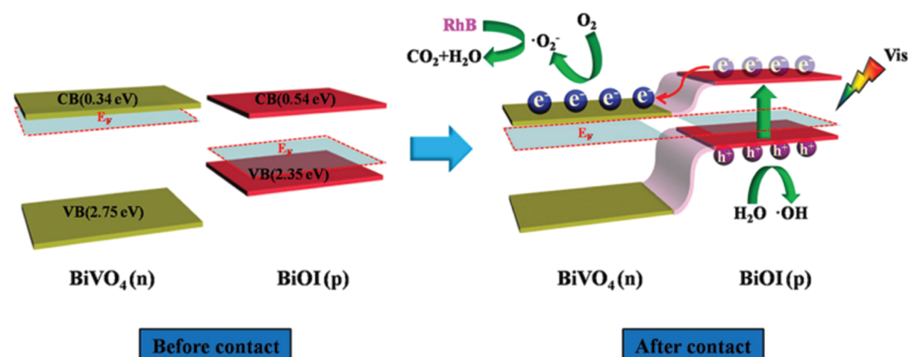


Figure 5. Schematic of formation of *p-n* junction and proposed charge separation process in the BiVO₄/BiOI core/shell heterostructures under visible-light irradiation. Reprinted with permission from [164], H. Huang, et al., *ACS Sustain. Chem. Eng.* 12, 3262 (2015). © 2015, American Chemical Society.

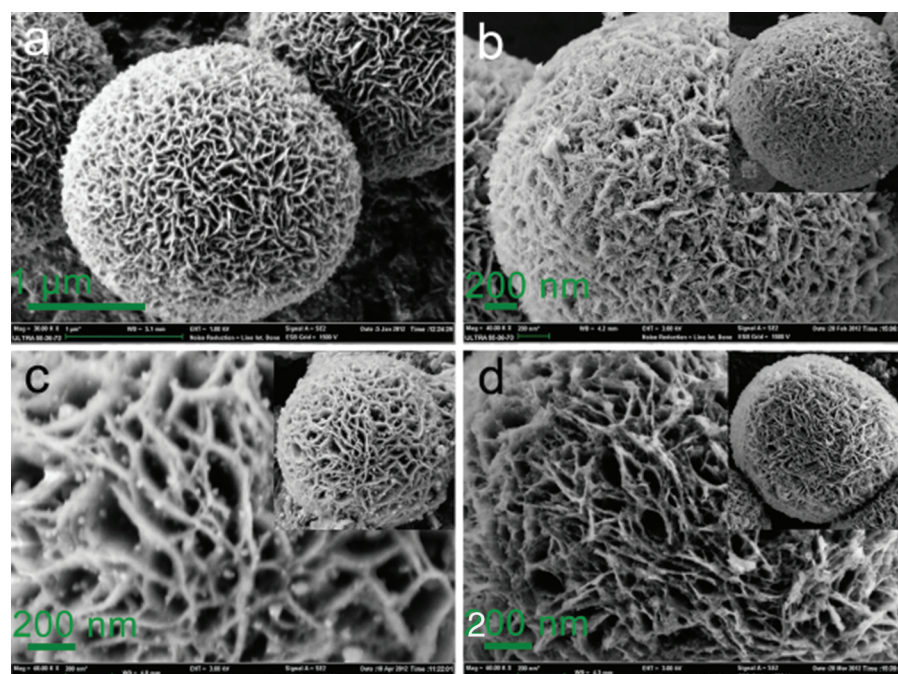


Figure 6. FE-SEM images of (a) the as-prepared Ti-doped BiOBr microsphere, (b) C-Ag, (c) P-Ag, and (d) T-3% Ag. Reprinted with permission from [165], G. Jiang, et al., *ACS Appl. Mater. Interfaces* 4, 4440 (2012). © 2012, American Chemical Society.

respect to the corresponding band edges shift. This shifting allows easy migration of the excited electrons from the conduction band of BiOI to that of BiVO₄ leaving behind the holes in the valence band of BiOI. This facilitates effective separation of the electron-hole pair resulting into high photocatalytic activity towards RhB and Phenol as compared to pure BiOI and BiVO₄ under visible light.

In order to efficiently separate the photogenerated electron-hole species BiOX compounds have also been associated with noble metals metal nanoparticles such as Au, Ag and Pt etc. As the BiOX shows *p*-type conductivity and lower Fermi level as compared the noble metals upon contact, the holes in the valance band edges of BiOX transfer to the noble metal until equilibrium is set up which results in the formation of a schottky barriers at the interface of the holes. The role of metal nanoparticles in the structure is to act as trap centre for the photogenerated electrons of BiOX upon irradiation, this interfacial charge transfer between BiOX and the metal nanoparticles effectively enhance the photocatalytic performance under visible light. Guohua et al.¹⁶⁵ prepared Ag/Ti-doped BiOBr by different approaches i.e., chemical reduction, photoreduction, thermal reduction and a facile solvothermal route. The composite prepared by facile solvothermal route was found to be more effective photocatalytic activity towards the RhB degradation under visible light. The photocatalyst exhibited flower like microsphere structure as shown in Figure 6.

This interaction between the light approaching the surface and the noble metal nanoparticles results in the collective oscillation of the excited free electron, this

phenomenon is known as surface Plasmon resonance. Apart from noble metal nanoparticles, some of the co-catalysts and sensitizer modified hybrids have been employed to accelerate the separation of the photogenerated electron-hole pair. In this regard, graphene,²⁷ NiO_x⁴ and RuO₂,⁵ have been utilized to facilitate the interfacial charge transfer and photocatalytic performance. Xiao et al.¹⁶⁶ for the first time synthesized Sn-doped BiOCl/reduced graphene oxide by a facile and efficient route. From Figure 7, it can be seen that the reduced graphene oxide and Sn-doped BiOCl coexist in the composite structure. Also, the Sn-doped BiOCl clusters are well dispersed on the reduced graphene oxide layers.

The as-prepared Sn-doped BiOCl/reduced graphene oxide composite exhibited excellent photocatalytic activity

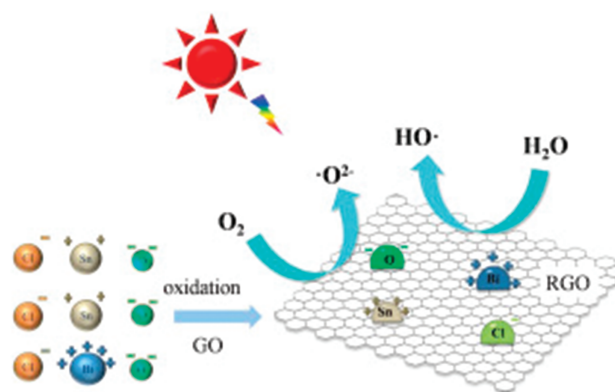


Figure 7. Incorporation of Sn-doped BiOCl on reduced graphene oxide film. Reprinted with permission from [166], X. Han, et al., *Mater. Lett.* 187, 154 (2017). © 2017, Elsevier.

towards RhB as compared to Sn-doped BiOCl under natural sunlight. Other examples of graphene doped BiOX composites have been listed in the Table II given above. Considering BiOCl, being a wide band gap semiconductor is UV activated just like TiO₂, apart from associating it with narrow band gap semiconductor, it can also be coupled with photosensitizers. In this context, Wang and coworkers¹⁶² introduced copper phthalocynaine as a photosensitizer to BiOCl through the liquid coating method. The as-prepared composite exhibited far superior almost 76 times photocurrent density as compared to the pure BiOCl under the simulated solar light.

4. INTRODUCTION OF DEFECT AND SOLID SOLUTIONS

One way of enhancing the separation of the photogenerated electron-hole pair and photocatalytic activity is due to the introduction of defects¹⁶⁷ and doping of the foreign atoms.¹⁰ The DFT calculations of BiOX reveal that the conduction band is dominated by Bi 6*p* orbitals, whereas the valence band is dominated by both X *np* (*n* = 3, 4 and 5 for Cl, Br and I) and O 2*p* orbitals. With the increase in the atomic number the halogen atoms the density peak of X *np* states moves towards the valence band top from the valence band resulting in the decrease of the band gap as we go from Cl to I. Various transition metals ions such as Fe¹⁶⁸ and Ti¹⁶⁹ as well as nonmetals such as I^{170, 171} have been utilized to dope with BiOX. Mn-doped BiOCl¹⁷² is one such example, where Mn²⁺ with ionic

radius of 0.080 nm incorporates well into BiOCl, as the size of the ionic radius of Mn and Bi ions is similar, hence this causes a red-shift in the absorption edge, resulting in a higher photocatalytic activity towards the degradation of malachite green under halogen lamp irradiation. Apart from metal ion doping, non-metal anionic doping was also found to be very effective in the enhancement of the photocatalytic activity. Zhang and coworkers,¹⁷³ reported that the doping of iodine in BiOI resulted in the tuning of the band structure and electronic properties. The composite exhibited higher photocatalytic activity towards MO degradation and NO removal under visible light.

Another way to continuously tune the band gap of the photocatalyst is to prepare the solid solutions. With the doping of metal or nonmetal ions and the defects, the energy states are isolated below and above the conduction and valence band. It has been reported that there is large amount of solubility among BiOX,¹⁷⁴ which offers the possibility to form BiOX-X solid solutions. In addition, on the basis of the theoretical calculations, the alloying effect in the BiOX solid solutions could potentially inhibit the recombination of the photogenerated electron-hole pair.¹⁷⁵ Till now various solid solutions have been synthesized.^{176–183} In this context, Xind et al.,¹⁸⁴ fabricated a series of 2D nanoplate like BiOBr_xI_{1-x} solutions via solvothermal route with exposed {001} facets with modulation of band gaps from 2.87 eV to 1.89 eV. From Figure 8(a), it can be seen that there is a discern red shift of the absorption edges as the values of *x* are varied (*X* = 1.0, 0.8, 0.5, 0.2, and 0.0), the color of the solid

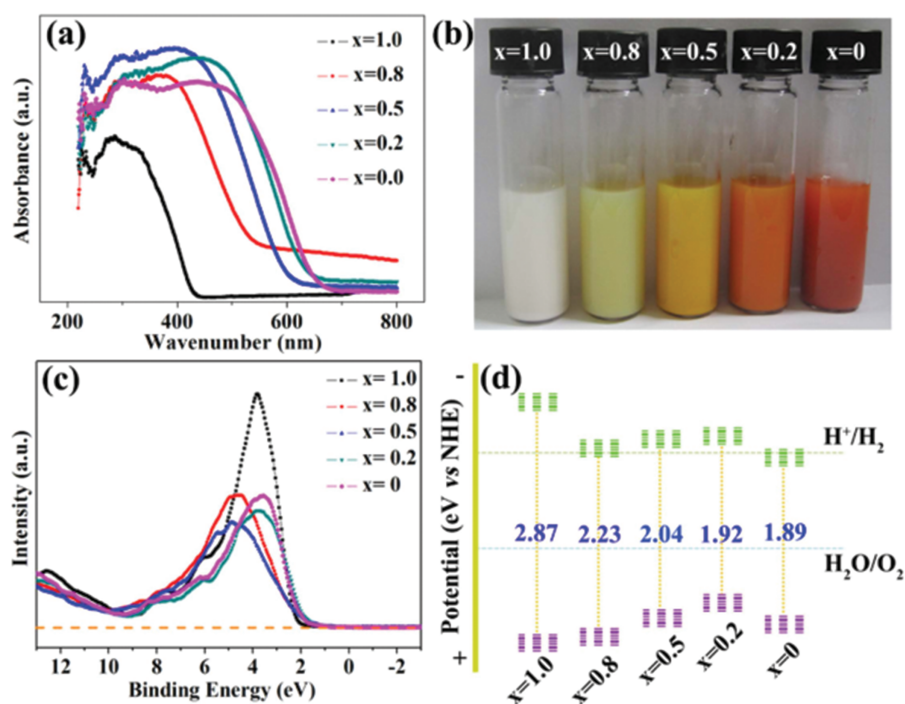


Figure 8. (a) UV-vis absorption spectra, (b) corresponding colors, (c) valence band spectra, (d) relative conduction band and valence band position of BiOBr_xI_{1-x}. Reprinted with permission from [184], X. Zhang, et al., *Sci. Rep.* 6, Article No. 22800 (2016). © 2016, Nature Publishing Group.

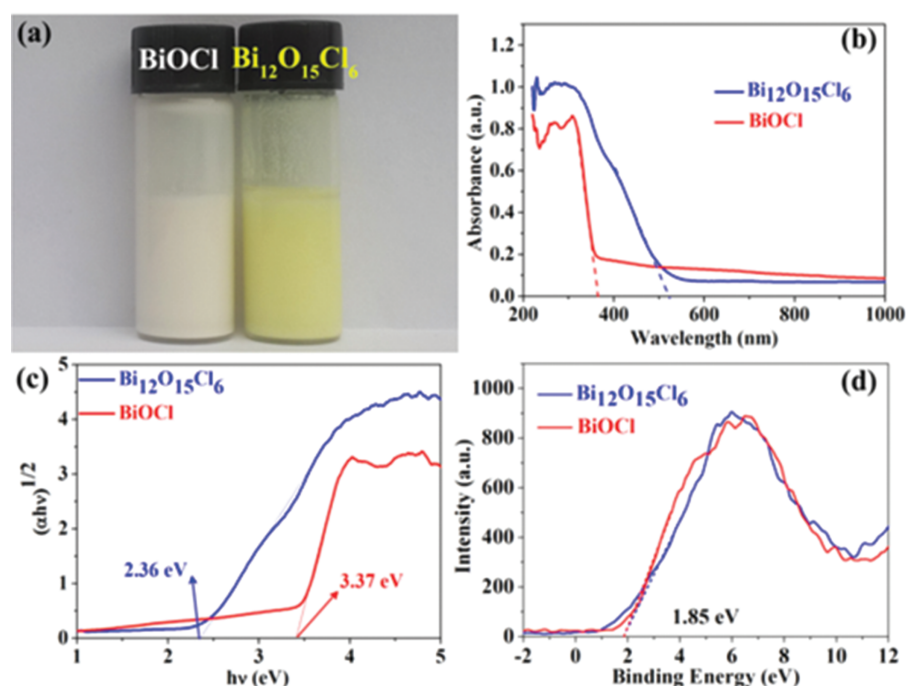


Figure 9. (a) Images of the $\text{Bi}_{12}\text{O}_{15}\text{Cl}_6$ nanosheets and BiOCl , (b) UV-vis diffuse reflectance spectrum, (c) the band gap values, estimated from the plotted curve of $(\alpha h\nu)^{1/2}$ versus $h\nu$, and (d) XPS valence band spectrum for $\text{Bi}_{15}\text{O}_{12}\text{Cl}_6$ and BiOCl . Reprinted with permission from [197], C. Y. Wang, et al., *ACS Appl. Mater. Interfaces* 8, 5320 (2016). © 2016, American Chemical Society.

solutions seem to be changing from white to red which also implies that the band gaps of the $\text{BiOBr}_x\text{I}_{1-x}$ solid solutions can be tuned precisely. Also the valence band of $\text{BiOBr}_x\text{I}_{1-x}$ nanoplate solid solutions was measured by XPS valence spectroscopy which shows the valence bands with the edge of the maximum energy at appropriately 2.32, 2.24, 2.0, 1.85 and 2.07 eV respectively as shown in Figure 8(c), it was found that $\text{BiOBr}_{0.8}\text{I}_{0.2}$ exhibited the maximum photocatalytic activity towards the photodegradation of RhB.

The optical, electronic and photocatalytic properties of a semiconductor are immensely influenced by their composition and phase structure. By varying the compositions and altering the elements other BiOX forms can be obtained such as $\text{Bi}_5\text{O}_7\text{I}$,^{185–187} BiOF ,¹⁸⁸ $\text{Na}_{0.5}\text{Bi}_{1.5}\text{O}_2\text{Cl}$,¹⁸⁹ PbBiO_2Br ,¹⁹⁰ $\text{Bi}_3\text{O}_4\text{Br}$,¹⁹¹ PbBiO_2Cl ,^{192, 193} CaBiO_2Cl ,¹⁹⁴ $\text{Bi}_{12}\text{O}_{17}\text{Cl}_2$,¹⁹⁵ $\text{Bi}_3\text{O}_4\text{Cl}$ ¹⁹⁶ etc. Chu et al.,¹⁹⁷ synthesized a novel $\text{Bi}_{12}\text{O}_{15}\text{Cl}_6$ nanosheets by facile solvothermal route followed by thermal treatment route. As shown in Figure 9, the colors of the corresponding BiOCl and $\text{Bi}_{12}\text{O}_{15}\text{Cl}_6$ are white and yellow, the UV-vis. DRS spectra revealed the band gaps of the as-prepared samples by the extrapolation of the linear Tauc region and they were found to be 2.36 eV and 3.37 eV for $\text{Bi}_{12}\text{O}_{15}\text{Cl}_6$ and BiOCl respectively. Because of the narrow band gap, $\text{Bi}_{12}\text{O}_{15}\text{Cl}_6$ nanosheets exhibited much higher photocatalytic activity towards the degradation of Bisphenol A which was 13.6 and 8.7 times faster than BiOCl and P25 under visible light respectively. Combination of BiOX with Aurivillius family $[\text{Bi}_2\text{O}_2][\text{A}_{n-1}\text{B}_n\text{O}_{3n+1}]$ results in the formation of novel

photocatalysts such as $\text{Bi}_4\text{TaO}_8\text{Cl}$ ¹⁹⁸ and $\text{Bi}_4\text{NbO}_8\text{Cl}$ ¹⁹⁹ etc. $\text{Bi}_4\text{NbO}_8\text{Cl}$ in terms of $[\text{Bi}_2\text{O}_2][\text{NbO}_4][\text{Bi}_2\text{O}_2][\text{Cl}]$, in which two dimensional $[\text{Bi}_2\text{O}_2]$, $[\text{NbO}_4]$ and $[\text{Cl}]$ slabs are oriented in a sequential layered structure. The internal electric field among the slabs is supposed to facilitate the separation of photogenerated species.

5. SUMMARY AND OUTLOOK

As visible light driven semiconductors, BiOX has shown promising photocatalytic applications. Various methods have been adopted to synthesize BIOX and to further enhance their photocatalytic activity, a large number of approaches have been adopted to facilitate the interfacial charge transfer and inhibition of the photogenerated electron-hole pair recombination. Moreover, three dominant approaches have been employed: (1) varying the multi-length scale of BiOX photocatalysts in different dimensions, i.e., 1D template nanofibres, 2D nanosheets, 3D hierarchical heterostructure and thin films. (2) Hybridization with other metals, nonmetals, semiconductors, co-catalyst etc. (3) Structural modifications by doping and introduction of defects, solid solutions etc. Palatably, for better efficiency of BiOX photocatalysts, the synergistic effect of several systems is required. For example, $\text{Ag}/\text{AgBr}/\text{BiOBr}$ hybrid,¹⁵⁸ a three component system serves the virtues of a plasmonic Ag/AgBr photocatalyst and AgBr/BiOBr composite photocatalyst, displaying highly enhanced photocatalytic activity for the sterilization of pathogenic organisms and dye degradation under visible

light irradiation. Although a lot of work on BiOX has been done, the research on BiOX is still in the early stages, and a lot can be explored in the future.

In some cases, BiOX fails to deliver the requirements to split water into H₂ because of confinement by their conduction band levels. Until now, BiOX is prominently focused on the degradation of organic pollutants. There are certain applications of BiOX such as CO₂ reduction and selective organic transformation, need to be addressed. As the photocatalytic activity of a semiconductor is dependent on its light responsive range and separation efficiency of photogenerated species, rational designing of BiOX based complex architecture systems is crucial. For instance, the periodic structures in the inverse opals can sufficiently enhance its light harvesting by multiple scattering, and the desired unintermitted pore tunnels could enhance the separation of photogenerated charge carriers, hence making it a capable candidate for next generation photocatalysts. Furthermore, with the help of voltage bias, it is captivating to study the photo-electrocatalysis of BiOX, which provides new opportunities to improve their photocatalytic properties.

For the development of novel photocatalysts, chemical modification of the existing materials into a novel material provides a versatile synthetic strategy. By adopting this approach, a class of well-defined nanostructures has been developed so far such as Bi₂WO₆ hollow microspheres¹⁸² and Bi₂S₃ superstructured materials.^{185–187} The web of Nanoscience and nanotechnology has brought new aspects and guidance to develop photocatalysts with higher efficiency and stability. With time, in-depth investigations in the field of BiOX have occurred, and numerous practical applications for environmental remediation have been established.

Acknowledgment: The authors gratefully acknowledge the support from the DST-NRDIO, Indo-Hungarian project (INT/HUN/P-06/2016, TÉT_15-IN-1-2016-0013) and WOG Technology, New Delhi, India.

References and Notes

- M. R. Hoffmann, S. T. Martin, W. Choi, and D. W. Bahnemann, *Chem. Rev.* 95, 69 (1995).
- C. C. Chen, W. H. Ma, and J. C. Zhao, *Chem. Soc. Rev.* 39, 4206 (2010).
- A. Fujishima and K. Honda, *Nature* 238, 37 (1972).
- F. E. Osterloh, *Chem. Mater.* 20, 35 (2008).
- A. Kudo and Y. Miseki, *Chem. Soc. Rev.* 38, 253 (2009).
- T. Inoue, A. Fujishima, S. Konishi, and K. Honda, *Nature* 277, 637 (1979).
- V. P. Indrakanti, J. D. Kubicki, and H. H. Schobert, *Energy Environ. Sci.* 2, 745 (2009).
- S. C. Roy, O. K. Varghese, M. Paulose, and C. A. Grimes, *ACS Nano* 4, 1259 (2010).
- A. L. Linsebigler, G. Lu, and J. T. Yates, *Chem. Rev.* 95, 735 (1995).
- X. B. Chen and S. S. Mao, *Chem. Rev.* 107, 2891 (2007).
- H. G. Yang, C. H. Sun, S. Z. Qiao, J. Zou, G. Liu, S. C. Smith, H. M. Cheng, and G. Q. Lu, *Nature* 453, 638 (2008).
- X. B. Chen, L. Liu, P. Y. Yu, and S. S. Mao, *Science* 331, 746 (2011).
- P. V. Kamat, *J. Phys. Chem. C* 116, 11849 (2012).
- K. Nakata and A. Fujishima, *J. Photochem. Photobiol. C* 13, 169 (2012).
- W. J. Wang, B. B. Huang, X. C. Ma, Z. Y. Wang, X. Y. Qin, X. Y. Zhang, Y. Dai, and M. H. Whangbo, *Chem.-Eur. J.* 19, 14777 (2013).
- W. F. Yao, X. H. Xu, H. Wang, J. T. Zhou, X. N. Yang, Y. Zhang, S. X. Shang, and B. B. Huang, *Appl. Catal. B* 52, 109 (2004).
- W. Wei, Y. Dai, and B. B. Huang, *J. Phys. Chem. C* 113, 5658 (2009).
- L. Zhou, W. Z. Wang, H. L. Xu, S. M. Sun, and M. Shang, *Chem.-Eur. J.* 15, 1776 (2009).
- H. F. Cheng, B. B. Huang, J. B. Lu, Z. Y. Wang, B. Xu, X. Y. Qin, X. Y. Zhang, and Y. Dai, *Phys. Chem. Chem. Phys.* 12, 15468 (2010).
- F. Amano, A. Yamakata, K. Nogami, M. Osawa, and B. Ohtani, *J. Am. Chem. Soc.* 130, 17650 (2008).
- L. W. Zhang, Y. J. Wang, H. Y. Cheng, W. Q. Yao, and Y. F. Zhu, *Adv. Mater.* 21, 1286 (2009).
- L. S. Zhang, H. L. Wang, Z. G. Chen, P. K. Wong, and J. S. Liu, *Appl. Catal. B* 106, 1 (2011).
- S. S. Yao, J. Y. Wei, B. B. Huang, S. Y. Feng, X. Y. Zhang, X. Y. Qin, P. Wang, Z. Y. Wang, Q. Zhang, X. Y. Jing, and J. Zhan, *J. Solid State Chem.* 182, 236 (2009).
- J. W. Tang, Z. G. Zou, and J. H. Ye, *Angew. Chem. Int. Ed.* 43, 4463 (2004).
- A. Kudo, K. Omori, and H. Kato, *J. Am. Chem. Soc.* 121, 11459 (1999).
- G. C. Xi and J. H. Ye, *Chem. Commun.* 46, 1893 (2010).
- R. Li, F. Zhang, D. Wang, J. Yang, M. Li, J. Zhu, X. Zhou, H. Han, and C. Li, *Nat. Commun.* 4, 1432 (2013).
- Y. Y. Liu, B. B. Huang, Y. Dai, X. Y. Zhang, X. Y. Qin, M. H. Jiang, and M. H. Whangbo, *Catal. Commun.* 11, 210 (2009).
- Y. Y. Liu, Z. Y. Wang, B. B. Huang, X. Y. Zhang, X. Y. Qin, and Y. Dai, *J. Colloid Interface Sci.* 348, 211 (2010).
- H. F. Cheng, B. B. Huang, K. S. Yang, Z. Y. Wang, X. Y. Qin, X. Y. Zhang, and Y. Dai, *ChemPhysChem* 11, 2167 (2010).
- Y. Y. Liu, Z. Y. Wang, B. B. Huang, K. S. Yang, X. Y. Zhang, X. Y. Qin, and Y. Dai, *Appl. Surf. Sci.* 257, 172 (2010).
- J. Geng, W. H. Hou, Y. N. Lv, J. J. Zhu, and H. Y. Chen, *Inorg. Chem.* 44, 8503 (2005).
- K. Zhang, C. Liu, F. Huang, C. Zheng, and W. Wang, *Appl. Catal. B: Environ.* 68, 125 (2006).
- X. Zhang and L. Zhang, *J. Phys. Chem. C* 114, 18198 (2010).
- X. Chang, J. Huang, C. Cheng, Q. Sui, W. Sha, G. Ji, S. Deng, and G. Yu, *Catal. Commun.* 11, 460 (2010).
- H. Cheng, B. Huang, P. Wang, Z. Wang, Z. Lou, J. Wang, X. Qin, X. Zhang, and Y. Dai, *Chem. Commun.* 47, 7054 (2011).
- X. Xiao and W. D. Zhang, *J. Mater. Chem.* 20, 5866 (2010).
- G. Li, F. Qin, R. Wang, S. Xiao, H. Sun, and R. Chen, *J. Colloid Interface Sci.* 409, 43 (2013).
- F. J. Maile, G. Pfaff, and P. Reynnders, *Prog. Org. Coat.* 54, 150 (2005).
- G. G. Briand and N. Burford, *Chem. Rev.* 99, 2601 (1999).
- N. Kijima, K. Matano, M. Saito, T. Oikawa, T. Konishi, H. Yasuda, T. Sato, and Y. Yoshimura, *Appl. Catal., A* 206, 237 (2001).
- C. H. Wang, C. L. Shao, Y. C. Liu, and L. N. Zhang, *Scr. Mater.* 59, 332 (2008).
- R. S. Yuan, C. Lin, B. C. Wu, and X. Z. Fu, *Eur. J. Inorg. Chem.* 2009, 3537 (2009).
- S. J. Wu, C. Wang, Y. F. Cui, T. M. Wang, B. B. Huang, X. Y. Zhang, X. Y. Qin, and P. Brault, *Mater. Lett.* 64, 115 (2010).

45. C. R. Michel, N. L. López Contreras, and A. H. MarfinezPreciado, *Sens. Actuators, B* 173, 100 (2012).
46. L. Q. Ye, L. Zan, L. Tian, T. Peng, and J. Zhang, *Chem. Commun.* 47, 6951 (2011).
47. D. Zhang, J. Li, Q. G. Wang, and Q. S. Wu, *J. Mater. Chem. A* 1, 8622 (2013).
48. X. F. Chang, J. Huang, C. Cheng, Q. Sui, W. Sha, G. B. Ji, S. B. Deng, and G. Yu, *Catal. Commun.* 11, 460 (2010).
49. X. Chang, M. A. Gondal, A. A. Al-Saadi, M. A. Ali, H. Shen, Q. Zhou, J. Zhang, M. Du, Y. Liu, and G. Ji, *J. Colloid Interface Sci.* 377, 291 (2012).
50. J. Jiang, K. Zhao, X. Y. Xiao, and L. Z. Zhang, *J. Am. Chem. Soc.* 134, 4473 (2012).
51. J. Y. Xiong, G. Cheng, G. F. Li, F. Qin, and R. Chen, *RSC Adv.* 1, 1542 (2011).
52. M. Shang, W. Z. Wang, and L. Zhang, *J. Hazard. Mater.* 167, 803 (2009).
53. L. Q. Ye, L. H. Tian, T. Y. Peng, and L. Zan, *J. Mater. Chem.* 21, 12479 (2011).
54. X. Zhang, Z. H. Ai, F. L. Jia, and L. Z. Zhang, *J. Phys. Chem. C* 112, 747 (2008).
55. X. Y. Qin, H. F. Cheng, W. J. Wang, B. B. Huang, X. Y. Zhang, and Y. Dai, *Mater. Lett.* 100, 285 (2013).
56. J. X. Xia, J. Zhang, S. Yin, H. M. Li, H. Xu, L. Xu, and Q. Zhang, *J. Phys. Chem. Solids* 74, 298 (2013).
57. J. M. Song, C. J. Mao, H. L. Niu, Y. H. Shen, and S. Y. Zhang, *Cryst. Eng. Comm.* 12, 3875 (2010).
58. L. P. Zhu, G. H. Liao, N. C. Bing, L. L. Wang, Y. Yang, and H. Y. Xie, *Cryst. Eng. Comm.* 12, 3791 (2010).
59. S. J. Peng, L. L. Li, P. N. Zhu, Y. Z. Wu, M. Srinivasan, S. G. Mhaisalkar, S. Ramakrishna, and Q. Y. Yan, *Chem.-Asian J.* 8, 258 (2013).
60. D. H. Wang, G. Q. Gao, Y. W. Zhang, L. S. Zhou, A. W. Xu, and W. Chen, *Nanoscale* 4, 7780 (2012).
61. J. Zhang, F. Shi, J. Lin, D. Chen, J. Gao, Z. Huang, X. Ding, and C. Tang, *Chem. Mater.* 20, 2937 (2008).
62. Z. H. Ai, W. Ho, S. Lee, and L. Z. Zhang, *Environ. Sci. Technol.* 43, 4143 (2009).
63. J. Xu, W. Meng, Y. Zhang, L. Li, and C. S. Guo, *Appl. Catal. B* 107, 355 (2011).
64. H. F. Cheng, B. B. Huang, Z. Y. Wang, X. Y. Qin, X. Y. Zhang, and Y. Dai, *Chem.-Eur. J.* 17, 8039 (2011).
65. Y. J. Chen, M. Wen, and Q. S. Wu, *Cryst. Eng. Comm.* 13, 3035 (2011).
66. J. X. Xia, S. Yin, H. M. Li, H. Xu, L. Xu, and Y. G. Xu, *Dalton Trans.* 40, 5249 (2011).
67. L. Zhang, X. F. Cao, X. T. Chen, and Z. L. Xue, *J. Colloid Interface Sci.* 354, 630 (2011).
68. D. Q. Zhang, M. C. Wen, B. Jiang, G. S. Li, and J. C. Yu, *J. Hazard. Mater.* 211–212, 104 (2012).
69. Y. C. Feng, L. Li, J. W. Li, J. F. Wang, and L. Liu, *J. Hazard. Mater.* 192, 538 (2011).
70. Y. N. Huo, J. Zhang, M. Miao, and Y. Jin, *Appl. Catal. B* 111–112, 334 (2012).
71. H. T. Tian, J. W. Li, M. Ge, Y. P. Zhao, and L. Liu, *Catal. Sci. Technol.* 2, 2351 (2012).
72. Y. Y. Li, J. S. Wang, H. C. Yao, L. Y. Dang, and Z. J. Li, *J. Mol. Catal. A: Chem.* 334, 116 (2011).
73. J. X. Xia, S. Yin, H. M. Li, H. Xu, Y. S. Yan, and Q. Zhang, *Langmuir* 27, 1200 (2011).
74. B. Zhang, G. Ji, M. A. Gondal, Y. Liu, X. Zhang, X. Chang, and N. Li, *J. Nanopart. Res.* 15, 1773 (2013).
75. L. Chen, S. F. Yin, R. Huang, Y. Zhou, S. L. Luo, and C. T. Au, *Catal. Commun.* 23, 54 (2012).
76. K. Zhang, J. Liang, S. Wang, J. Liu, K. X. Ren, X. Zheng, H. Luo, Y. J. Peng, X. Zou, X. Bo, J. H. Li, and X. B. Yu, *Cryst. Growth Des.* 12, 793 (2012).
77. Y. Q. Lei, G. H. Wang, S. Y. Song, W. Q. Fan, M. Pang, J. K. Tang, and H. J. Zhang, *Dalton Trans.* 39, 3273 (2010).
78. R. Hao, X. Xiao, X. X. Zuo, J. M. Nan, and W. D. Zhang, *J. Hazard. Mater.* 209–210, 137 (2012).
79. Y. Q. Lei, G. H. Wang, S. Y. Song, W. Q. Fan, and H. J. Zhang, *Cryst. Eng. Comm.* 11, 1857 (2009).
80. C. H. Deng and H. M. Guan, *Mater. Lett.* 107, 119 (2013).
81. G. Cheng, J. Y. Xiong, and F. J. Stadler, *New J. Chem.* 37, 3207 (2013).
82. X. Xiao and W. D. Zhang, *J. Mater. Chem.* 20, 5866 (2010).
83. J. Y. Xiong, Z. B. Jiao, G. X. Lu, W. Ren, J. H. Ye, and Y. P. Bi, *Chem.-Eur. J.* 19, 9472 (2013).
84. L. Zhu, Y. Xie, X. Zheng, X. Yin, and X. Tian, *Inorg. Chem.* 41, 4560 (2002).
85. J. Geng, W. H. Hou, Y. N. Lv, J. J. Zhu, and H. Y. Chen, *Inorg. Chem.* 44, 8503 (2005).
86. H. Deng, J. W. Wang, Q. Peng, X. Wang, and Y. D. Li, *Chem.-Eur. J.* 11, 6519 (2005).
87. J. Henle, P. Simon, A. Frenzel, S. Scholz, and S. Kaskel, *Chem. Mater.* 19, 366 (2007).
88. Z. T. Deng, D. Chen, B. Peng, and F. Q. Tang, *Cryst. Growth Des.* 8, 2995 (2008).
89. Z. T. Deng, F. Q. Tang, and A. J. Muscat, *Nanotechnol.* 19, 295705 (2008).
90. H. L. Peng, C. K. Chan, S. Meister, X. F. Zhang, and Y. Cui, *Chem. Mater.* 21, 247 (2009).
91. S. H. Cao, C. F. Guo, Y. Lv, Y. J. Guo, and Q. Liu, *Nanotechnol.* 20, 275702 (2009).
92. J. M. Ma, X. D. Liu, J. B. Lian, X. C. Duan, and W. J. Zheng, *Cryst. Growth Des.* 10, 2522 (2010).
93. A. Luz and C. Feldmann, *Solid State Sci.* 13, 1017 (2011).
94. K. L. Zhang, C. M. Liu, F. Q. Huang, C. Zheng, and W. D. Wang, *Appl. Catal. B* 68, 125 (2006).
95. Q. H. Mu, Q. H. Zhang, H. Z. Wang, and Y. G. Li, *J. Mater. Chem.* 22, 16851 (2012).
96. X. C. Zhang, X. X. Liu, C. M. Fan, Y. W. Wang, Y. F. Wang, and Z. H. Liang, *Appl. Catal. B* 132–133, 332 (2013).
97. Y. Y. Li, J. P. Liu, J. Jiang, and J. G. Yu, *Dalton Trans.* 40, 6632 (2011).
98. K. Li, Y. P. Tang, Y. L. Xu, Y. L. Wang, Y. N. Huo, H. X. Li, and J. P. Jia, *Appl. Catal. B* 140–141, 179 (2013).
99. L. Q. Ye, J. N. Chen, L. H. Tian, J. Y. Liu, T. Y. Peng, K. J. Deng, and L. Zan, *Appl. Catal. B* 130–131, 1 (2013).
100. K. W. Wang, F. L. Jia, Z. Zheng, and L. Z. Zhang, *Electrochem. Commun.* 12, 1764 (2010).
101. N. T. Hahn, S. Hoang, J. L. Self, and C. B. Mullins, *ACS Nano* 6, 7712 (2012).
102. Q. H. Wang, K. Kalantar-Zadeh, A. Kis, J. N. Coleman, and M. S. Strano, *Nat. Nanotechnol.* 7, 699 (2012).
103. M. Chhowalla, H. S. Shin, G. Eda, L. Li, K. P. Loh, and H. Zhang, *Nat. Chem.* 5, 263 (2013).
104. M. Q. Zhao, Q. Zhang, J. Q. Huang, and F. Wei, *Adv. Funct. Mater.* 22, 675 (2012).
105. J. H. Han, S. Lee, and J. Cheon, *Chem. Soc. Rev.* 42, 2581 (2013).
106. G. M. Whitesides and B. Grzybowski, *Sci.* 295, 2418 (2002).
107. M. A. Snyder and M. Tsapatsis, *Angew. Chem. Int. Ed.* 46, 7560 (2007).
108. D. R. Rolison, J. W. Long, J. C. Lythe, A. F. Fischer, C. P. Rhodes, T. M. McEvoy, M. E. Bourg, and A. M. Lubers, *Chem. Soc. Rev.* 38, 226 (2009).
109. Y. Li, Z. Y. Fu, and B. L. Su, *Adv. Funct. Mater.* 22, 4634 (2012).
110. Q. F. Zhang, E. Uchaker, S. L. Candelaria, and G. Z. Cao, *Chem. Soc. Rev.* 42, 3127 (2013).
111. H. Feng, Z. Xu, L. Wang, Y. Yu, D. R. G. Mitchell, D. Cui, X. Xu, J. Shi, T. Sannomia, Y. Du, W. Hao, and S. Dou, *ACS Appl. Mater. Interfaces* 50, 27592 (2015).

112. J. Zhang, F. Shi, J. Lin, D. Chen, J. Gao, Z. Huang, X. Huang, X. Ding, and C. Tang, *ACS Chem. Mater.* 20, 2937 (2008).
113. S. Y. Chai, Y. J. Kim, M. H. Jung, A. K. Chakraborty, D. Jung, and W. I. Lee, *J. Catal.* 262, 144 (2009).
114. S. Shamaila, A. K. L. Sajjad, F. Chen, and J. L. Zhang, *J. Colloid Interface Sci.* 356, 465 (2011).
115. L. Zhang, W. Z. Wang, L. Zhou, M. Shang, and S. M. Sun, *Appl. Catal. B* 90, 458 (2009).
116. X. F. Chang, G. Yu, J. Huang, Z. Li, S. F. Zhu, P. F. Yu, C. Cheng, S. B. Deng, and G. B. Ji, *Catal. Today* 53, 193 (2010).
117. A. K. Chakraborty, S. B. Rawal, S. Y. Han, S. Y. Chai, and W. I. Lee, *Appl. Catal. A* 407, 217 (2011).
118. H. H. Gan, G. K. Zhang, and Y. D. Guo, *J. Colloid Interface Sci.* 386, 373 (2012).
119. S. Shenawi-Khalil, V. Uvarov, E. Menes, I. Popov, and Y. Sasson, *Appl. Catal. A* 413–414, 1 (2012).
120. J. Zhang, J. X. Xia, S. Yin, H. M. Li, H. Xu, M. Q. He, L. Y. Huang, and Q. Zhang, *Colloids Surf. A* 420, 89 (2013).
121. T. B. Li, G. Chen, C. Zhou, Z. Y. Shen, R. C. Jin, and J. X. Sun, *Dalton Trans.* 40, 6751 (2011).
122. X. Xiao, R. Hao, M. Liang, X. X. Zuo, J. M. Nan, L. S. Li, and W. D. Zhang, *J. Hazard. Mater.* 233–234, 122 (2012).
123. H. F. Cheng, B. B. Huang, X. Y. Qin, X. Y. Zhang, and Y. Dai, *Chem. Commun.* 48, 97 (2012).
124. J. Cao, B. Xu, H. Lin, B. Luo, and S. Chen, *Catal. Commun.* 26, 204 (2012).
125. J. Cao, B. Y. Xu, H. L. Lin, B. D. Luo, and S. F. Chen, *Dalton Trans.* 41, 11482 (2012).
126. H. F. Cheng, B. B. Huang, Y. Dai, X. Y. Qin, and X. Y. Zhang, *Langmuir* 26, 6618 (2010).
127. H. F. Cheng, W. J. Wang, B. B. Huang, Z. Y. Wang, J. Zhan, X. Y. Qin, X. Y. Zhang, and Y. Dai, *J. Mater. Chem. A* 1, 7131 (2013).
128. L. L. Chen, D. L. Jiang, T. He, Z. D. Wu, and M. Chen, *Cryst. Eng. Comm.* 15, 7556 (2013).
129. L. Kong, Z. Jiang, H. H. Lai, R. J. Nicholls, T. Xiao, M. O. Jones, and P. P. Edwards, *J. Catal.* 293, 116 (2012).
130. Y. Li, Y. Liu, E. Uchaker, Q. Zhang, S. Sun, J. Wang, Y. Huang, J. Li, and G. Cao, *J. Mater. Chem. A* 1, 7949 (2013).
131. S. Shenawi-Khalil, V. Uvarov, S. Fronton, I. Popov, and Y. Sasson, *J. Phys. Chem. C* 116, 11004 (2012).
132. J. Cao, B. Xu, B. Luo, H. Lin, and S. Chen, *Catal. Commun.* 13, 63 (2011).
133. J. Fu, Y. L. Tian, B. B. Chang, F. N. Xi, and X. P. Dong, *J. Mater. Chem.* 22, 21159 (2012).
134. J. Di, J. X. Xia, S. Yin, H. Xu, M. Q. He, H. M. Li, L. Xu, and Y. P. Jiang, *RSC Adv.* 3, 19624 (2013).
135. X. Zhang, L. Z. Zhang, T. F. Xie, and D. J. Wang, *J. Phys. Chem. C* 113, 7371 (2009).
136. G. P. Dai, J. G. Yu, and G. Liu, *J. Phys. Chem. C* 115, 7339 (2011).
137. J. Jiang, X. Zhang, P. B. Sun, and L. Z. Zhang, *J. Phys. Chem. C* 115, 20555 (2011).
138. P. Li, X. Zhao, C. J. Jia, H. G. Sun, L. M. Sun, X. F. Cheng, L. Liu, and W. L. Fan, *J. Mater. Chem. A* 1, 3421 (2013).
139. K. H. Reddy, S. Martha, and K. M. Parida, *Inorg. Chem.* 52, 6390 (2013).
140. J. Cao, X. Li, H. L. Lin, S. F. Chen, and X. L. Fu, *J. Hazard. Mater.* 239–240, 316 (2012).
141. L. Chen, S. F. Yin, S. L. Luo, R. Huang, Q. Zhang, T. Hong, and P. C. T. Au, *Ind. Eng. Chem. Res.* 51, 6760 (2012).
142. Y. Y. Li, J. S. Wang, H. C. Yao, L. Y. Dang, and Z. J. Li, *Catal. Commun.* 12, 660 (2011).
143. D. F. Hou, X. L. Hu, P. Hu, W. Zhang, M. F. Zhang, and Y. H. Huang, *Nanoscale* 5, 9764 (2013).
144. D. Jiang, L. Chen, J. Zhu, M. Chen, W. Shi, and J. Xie, *Dalton Trans.* 42, 15726 (2013).
145. L. Kong, Z. Jiang, T. C. Xiao, L. F. Lu, M. O. Jones, and P. P. Edwards, *Chem. Commun.* 47, 5512 (2011).
146. C. L. Yu, J. C. Yu, C. F. Fan, H. R. Wen, and S. J. Hu, *Mater. Sci. Eng. B* 166, 213 (2010).
147. S. X. Weng, B. B. Chen, L. Y. Xie, Z. Y. Zheng, and P. Liu, *J. Mater. Chem. A* 1, 3068 (2013).
148. H. Liu, W. R. Cao, Y. Su, Y. Wang, and X. H. Wang, *Appl. Catal. B* 111–112, 271 (2012).
149. G. H. Jiang, R. J. Wang, X. H. Wang, X. G. Xi, R. B. Hu, Y. Zhou, S. Wang, T. Wang, and W. X. Chen, *ACS Appl. Mater. Interfaces* 4, 4440 (2012).
150. L. F. Lu, L. Kong, Z. Jiang, H. H. C. Lai, T. C. Xiao, and P. P. Edwards, *Catal. Lett.* 142, 771 (2012).
151. H. F. Cheng, B. B. Huang, P. Wang, Z. Y. Wang, Z. Z. Lou, J. P. Wang, X. Y. Qin, X. Y. Zhang, and Y. Dai, *Chem. Commun.* 2011, 47, 7054 (2011).
152. W. Xiong, Q. D. Zhao, X. Y. Li, and D. K. Zhang, *Catal. Commun.* 16, 229 (2011).
153. L. Q. Ye, J. Y. Liu, C. Q. Gong, L. H. Tian, T. Y. Peng, and L. Zan, *ACS Catal.* 2, 1677 (2012).
154. F. D. Gao, D. W. Zeng, Q. W. Huang, S. Q. Tian, and C. S. Xie, *Phys. Chem. Chem. Phys.* 14, 10572 (2012).
155. Z. H. Ai, W. Ho, and S. Lee, *J. Phys. Chem. C* 115, 25330 (2011).
156. X. M. Tu, S. L. Luo, G. X. Chen, and J. H. Li, *Chem.-Eur. J.* 18, 14359 (2012).
157. S. Y. Song, W. Gao, X. Wang, X. Y. Li, D. P. Liu, Y. Xing, and H. J. Zhang, *Dalton Trans.* 41, 10472 (2012).
158. H. Liu, W. R. Cao, Y. Su, Z. Chen, and Y. Wang, *J. Colloid Interface Sci.* 398, 161 (2013).
159. M. H. Su, C. He, L. F. Zhu, Z. J. Sun, C. Shan, Q. Zhang, D. Shu, R. L. Qiu, and Y. Xiong, *J. Hazard. Mater.* 229–230, 72 (2012).
160. Y. Wang, K. Deng, and L. Zhang, *J. Phys. Chem. C* 115, 14300 (2011).
161. L. Q. Ye, X. D. Liu, Q. Zhao, H. Q. Xie, and L. Zan, *J. Mater. Chem. A* 1, 8978 (2013).
162. L. Zhang, W. Z. Wang, S. M. Sun, Y. Y. Sun, E. P. Gao, and J. Xu, *Appl. Catal. B* 132–133, 315 (2013).
163. L. Q. Ye, C. Q. Gong, J. Y. Liu, L. H. Tian, T. Y. Peng, K. J. Deng, and L. Zan, *J. Mater. Chem.* 22, 8354 (2012).
164. H. Huang, Y. He, X. Du, P. K. Chu, and Y. Zhang, *ACS Sustain. Chem. Eng.* 12, 3262 (2015).
165. G. Jiang, R. Wang, X. Wang, X. Xi, R. Hu, Y. Zhou, S. Wang, T. Wang, and W. Cheng, *ACS Appl. Mater. Interfaces* 4, 4440 (2012).
166. X. Han, S. Dong, J. Sun, K. Wang, W. Zhang, and J. Sun, *Mater. Lett.* 187, 154 (2017).
167. X. Y. Pan, M. Q. Yang, X. Z. Fu, N. Zhang, and Y. J. Xu, *Nanoscale* 5, 3601 (2013).
168. Z. Liu, B. Wu, Y. Zhu, D. Yin, and L. Wang, *Catal. Lett.* 142, 1489 (2012).
169. G. Jiang, X. Wang, Z. Wei, X. Li, X. Xi, R. Hu, B. Tang, R. Wang, S. Wang, T. Wang, and W. Chen, *J. Mater. Chem. A* 1, 2406 (2013).
170. K. Zhang, D. Zhang, J. Liu, K. Ren, H. Luo, Y. Peng, G. Li, and X. Yu, *Cryst. Eng. Comm.* 14, 700 (2012).
171. B. Zhang, G. B. Ji, Y. S. Liu, M. A. Gondal, and X. F. Chang, *Catal. Commun.* 36, 25 (2013).
172. B. Pare, B. Sarwan, and S. B. Jonnalagadda, *Appl. Surf. Sci.* 258, 247 (2011).
173. X. Zhang and L. Z. Zhang, *J. Phys. Chem. C* 114, 18198 (2010).
174. E. Keller and V. Kramer, *Z. Naturforsch., B: Chem. Sci.* 60, 1255 (2005).
175. H. J. Zhang, L. Liu, and Z. Zhou, *Phys. Chem. Chem. Phys.* 14, 1286 (2012).
176. W. D. Wang, F. Q. Huang, and X. P. Lin, *Scr. Mater.* 56, 669 (2007).
177. W. D. Wang, F. Q. Huang, X. P. Lin, and J. H. Yang, *Catal. Commun.* 9, 8 (2008).
178. S. Shenawi-Khalil, V. Uvarov, Y. Kritsman, E. Menes, I. Popov, and Y. Sasson, *Catal. Commun.* 12, 1136 (2011).

179. Y. Y. Liu, W. J. Son, J. B. Lu, B. B. Huang, Y. Dai, and M. H. Whangbo, *Chem.-Eur. J.* 17, 9342 (2011).
180. Z. F. Jia, F. M. Wang, F. Xin, and B. Q. Zhang, *Ind. Eng. Chem. Res.* 50, 6688 (2011).
181. F. Dong, Y. J. Sun, M. Fu, Z. B. Wu, and S. C. Lee, *J. Hazard. Mater.* 219–220, 26 (2012).
182. H. Gnaïem and Y. Sasson, *ACS Catal.* 3, 186 (2013).
183. K. Ren, J. Liu, J. Liang, K. Zhang, X. Zheng, H. Luo, Y. Huang, P. Liu, and X. Yu, *Dalton Trans.* 42, 9706 (2013).
184. X. Zhang, C. Y. Wang, L. W. Wang, G. X. Huang, W. K. Wang, and H. Q. Yu, *Sci. Rep.* 6, Article No. 22800 (2016).
185. S. M. Sun, W. Z. Wang, L. Zhang, L. Zhou, W. Z. Yin, and M. Shang, *Environ. Sci. Technol.* 43, 2005 (2009).
186. X. Xiao, C. Liu, R. P. Hu, X. X. Zuo, J. M. Nan, L. S. Li, and L. S. Wang, *J. Mater. Chem.* 22, 22840 (2012).
187. J. Cao, X. Li, H. Lin, B. Xu, B. Luo, and S. Chen, *Mater. Lett.* 76, 181 (2012).
188. W. Y. Su, J. Wang, Y. X. Huang, W. J. Wang, L. Wu, X. X. Wang, and P. Liu, *Scr. Mater.* 62, 345 (2010).
189. X. P. Lin, Z. C. Shan, K. Q. Li, W. D. Wang, J. H. Yang, and F. Q. Huang, *Solid State Sci.* 9, 944 (2007).
190. Z. C. Shan, W. D. Wang, X. P. Lin, H. M. Ding, and F. Q. Huang, *J. Solid State Chem.* 181, 1361 (2008).
191. J. L. Wang, Y. Yu, and L. Z. Zhang, *Appl. Catal. B* 136–137, 112 (2013).
192. S. Fuldner, P. Pohla, H. Bartling, S. Dankesreiter, R. Stadler, M. Gruber, A. Pfitzner, and B. König, *Green Chem.* 13, 640 (2011).
193. Z. C. Shan, X. P. Lin, M. L. Liu, H. M. Ding, and F. Q. Huang, *Solid State Sci.* 11, 1163 (2009).
194. R. Shi, T. G. Xu, Y. F. Zhu, and J. Zhou, *Cryst. Eng. Comm.* 14, 6257 (2012).
195. X. Y. Xiao, J. Jiang, and L. Z. Zhang, *Appl. Catal. B* 142–143, 487 (2013).
196. X. P. Lin, T. Huang, F. Q. Huang, W. D. Wang, and J. L. Shi, *J. Phys. Chem. B* 110, 24629 (2006).
197. C. Y. Wang, X. Zhang, X. N. Song, W. K. Wang, and H. Q. Yu, *ACS Appl. Mater. Interfaces* 8, 5320 (2016).
198. S. S. M. Bhat and N. G. Sundaram, *RSC Adv.* 3, 14371 (2013).
199. X. P. Lin, T. Huang, F. Q. Huang, W. D. Wang, and J. L. Shi, *J. Mater. Chem.* 17, 2145 (2007).
200. X. Jin, L. Ye, H. Xie, and G. Chen, *Coord. Chem. Rev.* 349, 84 (2017).
201. H. Zhao, F. Tian, R. Wang, and R. Chen, *Adv. Sci. Eng.* 3, 3 (2014).
202. D. S. Bhachu, S. J. A. Moniz, S. Sathasivam, D. O. Scanlon, A. Walsh, S. M. Bawaked, M. Mokhtar, A. Y. Obaid, I. P. Parkin, J. Tang, and C. J. Carmalt, *Chem. Sci.* 7, 4832 (2016).
203. J. Di, J. Xia, H. Li, S. Guo, and S. Dai, *Nano Energ.* 41, 172 (2017).
204. L. Ye, J. Liu, Z. Jiang, T. Peng, and L. Zan, *Appl. Catal. B Environ.* 142–143, 1 (2013).
205. W. Liu, Y. Shang, A. Zhu, P. Tan, Y. Liu, L. Oiao, D. Chu, X. Xiong, and J. Pan, *J. Mater. Chem. A* 5, 12542 (2017).
206. A. Han, J. Sun, G. K. Chuah, and S. Jaenicke, *RSC Adv.* 7, 145 (2017).

Received: 9 September 2017. Accepted: 5 January 2018.